

A Modified Borel Summation Technique

David Leonard and Paul Mansfield

Centre for Particle Theory, Durham University, Durham, DH1 3LE, UK

E-mail: david.leonard@durham.ac.uk, p.r.w.mansfield@durham.ac.uk

Abstract. We compare and contrast three different perturbative expansions for the quartic anharmonic oscillator wavefunction and apply a modified Borel summation technique to determine the energy eigenvalues. In the first two expansions this provides the energy eigenvalues directly however in the third method we tune the wavefunctions to achieve the correct large x behaviour as first illustrated in [1]. This tuning technique allows us to determine the energy eigenvalues up to an arbitrary level of accuracy with remarkable efficiency. We give numerical evidence to explain this behaviour. We also refine the modified Borel summation technique to improve its accuracy. The main sources of error are investigated with reasonable error corrections calculated.

1. Introduction

Quantum Field Theory (QFT) is our most successful mathematical framework for describing the fundamental laws of physics. Despite this we still have few tools to calculate physical quantities in many models. Perturbation theory is probably the most important technique available to calculate such quantities however perturbative expansions are often divergent within their region of applicability. In addition some physical properties are not correctly reflected in perturbative expansions. For example, the renormalisation group implies that energy eigenvalues in Yang-Mills theory cannot be solved for perturbatively.

One technique that has been of interest in both the Schrödinger representation of quantum field theory and quantum mechanics is a modified type of Borel resummation [2][3][4][5]. The aim of this paper is to explore this particular method of resummation. It is important to test and develop the accuracy of our technique in a theory with known results so that we can confidently apply it to problems in which other techniques fail. Since energy eigenvalues are already known for the quantum mechanical anharmonic oscillator to a high degree of accuracy (e.g. [1][6] and references therein), we shall apply the resummation technique to this problem. That is we look for solutions to

$$-\frac{d^2\Psi}{dx^2} + \rho x^2\Psi + gx^4\Psi = E\Psi \quad (1)$$

$$\lim_{|x|\rightarrow\infty} \Psi = 0 \quad (2)$$

where x is defined along the real axis and we choose units in which $\hbar = 2m = 1$. We will generate three different perturbative expansions of the quartic anharmonic oscillator wavefunction as follows:

- An expansion in the coupling, g (Bender Wu expansion)
- An expansion in Planck's constant, \hbar (the semi classical expansion)
- An expansion in powers of x

In the first two approaches we take a perturbative expansion of the energy eigenvalue and directly resum to find an approximate result. In the third method we resum the large x behaviour of the wavefunction. This provides a variational technique in which the energy is tuned to ensure the correct boundary condition (2) is observed. This technique is remarkably efficient and provides energy eigenvalues up to an arbitrary level of accuracy as first illustrated in [1]. We shall apply the modified Borel resummation technique to provide further explanation as to why this method is so efficient.

The method of resummation we shall employ allows us to extract the small s properties from an asymptotic expansion which is only valid for large s . Therefore consider an asymptotic expansion of a function $f(s)$ in inverse powers of s :

$$f(s) \approx a_0 + \frac{c_1}{s} + \frac{c_2}{s^2} + \frac{c_3}{s^3} + \frac{c_4}{s^4} + \frac{c_5}{s^5} + \dots \quad (3)$$

We analytically continue $f(s)$ into the complex s plane, then Cauchy's theorem relates the large s to small $s = s_0$ behaviour of $f(s)$ via the integral

$$L(\lambda) = \int_C ds \frac{e^{\lambda(s-s_0)}}{s-s_0} f(s) \quad (4)$$

where C is a large circular contour centred on the origin. We only assume $f(s)$ to be analytic in the half plane $\Re(s-s_0) \geq 0$. Any singularity contributions to (4) in the half plane $\Re(s-s_0) < 0$ are exponentially dampend by λ so that $\lim_{\lambda \rightarrow \infty} L(\lambda) = f(s_0)$.

We approximate $L(\lambda)$ using a truncated version of the asymptotic expansion (3) and expanding the $s-s_0$ denominator in powers of s_0/s truncated to some order P . Thus we define

$$L_N(\lambda) = \int_C ds e^{\lambda(s-s_0)} \sum_{p=0}^P \frac{s_0^p}{s^{p+1}} \sum_{n=0}^N \frac{c_n}{s^n} \quad (5)$$

$$= \sum_{n=0}^N \sum_{p=0}^P c_n \frac{e^{-\lambda s_0} s_0^p \lambda^{n+p}}{\Gamma(n+p+1)} \approx L(\lambda). \quad (6)$$

where in completing the integral we used the identity $\int_C ds s^{-n} \exp(\lambda s) = 2\pi i \lambda^{n-1} / \Gamma(n)$ for $n < 0$. The introduction of the Gamma functions in this series improves the convergence of the original asymptotic expansion. We note however that the $L_N(\lambda)$ is only a good approximation to $L(\lambda)$ within a limited range of λ . For sufficiently large λ the series will be dominated by the highest powers of λ and exhibits a rapidly increasing or decreasing behaviour depending on the sign of the coefficient. We also note the similarity of this method to that of Borel summation. The Borel transform of

an asymptotic series results in the introduction of an additional $1/n!$ factor in each c_n . The Borel procedure however requires us to analytically continue the Borel transformed series before inversion. This is accomplished via techniques such as Padé approximants or conformal mapping. The advantage of our technique is that this analytic continuation is encoded in the contour integral.

We take λ as large as practicably possible with the constraint that $L_N(\lambda)$ be a good approximation to $L(\lambda)$. This is best achieved by requiring maximal $\lambda = \lambda_M$ such that $L_N(\lambda)$ differs from $L_{N-1}(\lambda)$ by no more than a set amount. In this paper we will choose λ_M so that they differ by no more than 10^{-3} percent. More terms (greater N) allows for a larger λ and therefore better dampening of any singularity contributions.

One method for increasing the singularity dampening for a given N is to introduce a new parameter, α by replacing $f(s)$ with $f(s^\alpha)$ and s_0 with $s_0^{1/\alpha}$ in $L(\lambda)$. For $\alpha > 1$ the size of the last term in L_N relative to its penultimate term L_{N-1} is reduced due to the gamma function in (5). This allows us to take a larger value of λ whilst $L_N(\lambda)$ remains a good approximation to $L(\lambda)$. Increasing α however causes singularities of f to be rotated about the origin. For α too large the singularities enter the half plane $\Re(s - s_0) \geq 0$ at which point they are no longer exponentially suppressed. $L(\lambda)$ will then exhibit oscillations resulting from these singularity contributions. We therefore take α to be as large as possible but still ensuring $L_N(\lambda)$ is monotonic as a function of λ for $\lambda < \lambda_M$. The technique originally (i.e. without the introduction of α) only worked for functions which are analytic in the half plane $\Re(s - s_0) \geq 0$. With the introduction of α we could also consider functions in which $f(s)$ has singularities with $\Re(s - s_0) \geq 0$. By reducing $\alpha < 1$ we can rotate these singularities back into the half plane $\Re(s - s_0) < 0$ where they become exponentially dampened.

In all three approaches we will solve the anharmonic oscillator ground state by writing $\Psi = e^W$ since the ground state of any quantum mechanical system has no nodes. In the case of the quartic anharmonic oscillator (1), the potential and boundary condition are even in x . We therefore expand W in the form $W = \sum_{n=1}^{\infty} a_n x^{2n}$. Substituting this expansion into the differential equation (1) and comparing coefficients of the x^{2n} we get relations between the a_n as follows

$$-2a_1 = E, \quad -12a_2 - 4a_1^2 + \rho = 0, \quad -30a_3 - 16a_1a_2 + g = 0 \quad (7)$$

and for $n \geq 3$

$$a_{n+1} = - \left(\sum_{m=1}^n 4m(n-m+1)a_m a_{n-m+1} \right) / (2(n+1)(2n+1)). \quad (8)$$

The equation (8) allows us to find a_{n+1} in terms of the a_m with $m \leq n$. We could therefore solve all of the a_n in terms of a_1 , a_2 and a_3 . In turn these first three coefficients are determined by the physical parameters E , ρ and g via (7). However for a given ρ and g only specific values of E allow the solution to satisfy the boundary condition (2). In sections 2, 3 and 4 we propose different methods for eliminating this final degree of freedom.

2. Bender Wu Expansion

Bender and Wu [7] showed how to construct the ground state energy by summing all connected Feynman diagrams with no external legs. In general a Feynman diagram with $2n$ external legs has at least $n - 1$ vertices. So we ensure that an x^{2n} term is at least order $n - 1$ in the coupling by making the expansion $a_n = \sum_{m=n-1}^{\infty} a_{n,m} g^m$. This is a similar approach to another method outlined by Bender and Wu in the same paper. We substitute this coupling expansion into the above relations between the a_n and compare coefficients of g^n . The first coefficient is given by $a_{1,0}^2 = 1/4$ which requires a choice of sign for $a_{1,0}$. In keeping with the Bender Wu methods [7] we choose a negative sign. In [1] we showed that this sign choice is required to ensure the correct boundary condition (2).

Having made the choice for $a_{1,0}$, the remaining coefficients are uniquely determined. We first find each $a_{n,n-1}$ by looking at the g^{n-1} coefficient in (7) and (8). The g^n coefficients give $a_{n,n}$ then the g^{n+1} coefficients give the $a_{n,n+1}$ etc. At each stage we are substituting in the previous solutions. Eventually we can find each a_n up to any order in g . Of course the coefficients will also depend on ρ however for the purpose of this section we set $\rho = 1$ without loss of generality since the eigenvalues for arbitrary ρ may be reproduced via a form of Symanzik scaling [8].

We now have a solution for the ground state wavefunction of (1) as the exponential of a power series in x and g . The energy eigenvalue is computed from a_1 using (7) as a power series in g . This gives the well known [7][9][10] Rayleigh Schrödinger perturbation expansion for $E(g)$,

$$E = 1 + \frac{3}{4}g - \frac{21}{16}g^2 + \frac{333}{64}g^3 - \frac{30885}{1024}g^4 + \frac{916731}{4096}g^5 - \frac{65518401}{32768}g^6 + \dots(9)$$

This expansion has a zero radius of convergence as can be seen from the asymptotic form of the $a_{1,n}$ coefficients at large n as given by Bender Wu [7]. It has been used to generate some energy eigenvalues via a Borel resummed Padé approximants technique [11][12] although many other techniques have been used to find the energy eigenvalues more accurately and efficiently e.g. [1][13][14][15][16][17][18].

We will apply our resummation method to $E(g)$ in an attempt to get meaningful results for non zero values of g . To do this we analytically continue g in the complex $s = 1/g$ plane. We write $s_0 = 1/g$ and $c_n = -2a_{1,n}$ then apply the contour integral technique so that $L_N(\lambda)$ in (5) approximates the energy.

The results generated via our resummation method are listed in figure 1 and compared to the results as generated by the method [1]. We label the eigenvalues generated by [1] E_{best} since they are accurate to within the number of significant figures expressed. The seemingly strange choices for g that we use becomes more natural in the semi classical expansion as outlined in the next section. We use the same values of g in both sections to allow comparison.

The results for small g are quite impressive with errors in the region of 10^{-3} to 10^{-4} percent however for larger g the results are less impressive with the error approximately

g	α_M	λ_M	L_{30}	E_{best}	Error (%)
0.05783	1.6398	2.9266	1.0397406	1.0397505	0.00095
0.13458	2.4250	7.6353	1.0846489	1.0846523	0.00031
0.23702	2.8159	10.4624	1.1359213	1.1359237	0.00021
0.37556	2.8160	9.9602	1.1952265	1.1952286	0.00017
0.56672	2.8160	9.6275	1.2649090	1.2649111	0.00017
0.83794	2.8159	9.3800	1.3483970	1.3483997	0.00020
1.23759	2.8160	9.1841	1.4509422	1.4509525	0.00071
1.85793	2.8160	9.0197	1.5810649	1.5811388	0.00467
2.89469	2.8160	8.8769	1.7536476	1.7541160	0.02671
4.83194	2.8160	8.7472	1.9974138	2.0000000	0.12948
9.19266	2.8160	8.6252	2.3766424	2.3904572	0.58127
23.50256	2.8160	8.5039	3.0767794	3.1622777	2.77882
206.09853	2.8160	8.3641	5.1098167	6.3245553	23.77265

Figure 1. Results for resummation of E in the coupling.

23.8% for the largest value of g .

Figure 2a (a small g example) shows the expected behaviour of $L_{29}(\lambda)$ and $L_{30}(\lambda)$ with $P = 50$. For sufficiently large λ the two curves become a good approximation to $L(\lambda)$ and we see a flattening of the curve. For λ sufficiently large we notice an appreciable divergence of the two curves. Figure 2b where g is relatively large has somewhat different behaviour. Here we notice that the curves have not started to flatten before they appreciably diverge. For these larger g we need more terms (greater N) in the expansion so that we may consider larger λ where the curve starts to flatten. Additionally we note that this curve exhibits oscillatory behaviour although remains monotonic. When we introduced the requirement for the curve to be monotonic we assumed that a singularity contribution would consist of an exponentially weighted sinusoidal correction to a flat curve. In this case we do not have sufficient terms to consider λ in the region where it becomes flat but instead are considering a region of the curve where it is still appreciably increasing. If we considered more terms with this value of α we may well find our monotonic condition is violated. Given the behaviour observed in figure 2b it is not surprising that we have such a large error.

In the next subsection we show that $\ddagger E \sim g^{1/3}$. Therefore as $g \rightarrow \infty$ or equivalently $s_0 \rightarrow 0$ we notice that E has a singularity. It is this singularity that is causing difficulty in the resummation process since we need larger λ for large g to ensure it is damped sufficiently. This in turn requires a larger N . The problems no doubt could be solved if we took a sufficient number of terms in the expansion of E however this would be at the expense of greater computing resources. In the next subsection we outline a more

\ddagger This can be seen by Symanzik scaling of the Hamiltonian [8]. The infinite coupling limit has been calculated in [19].

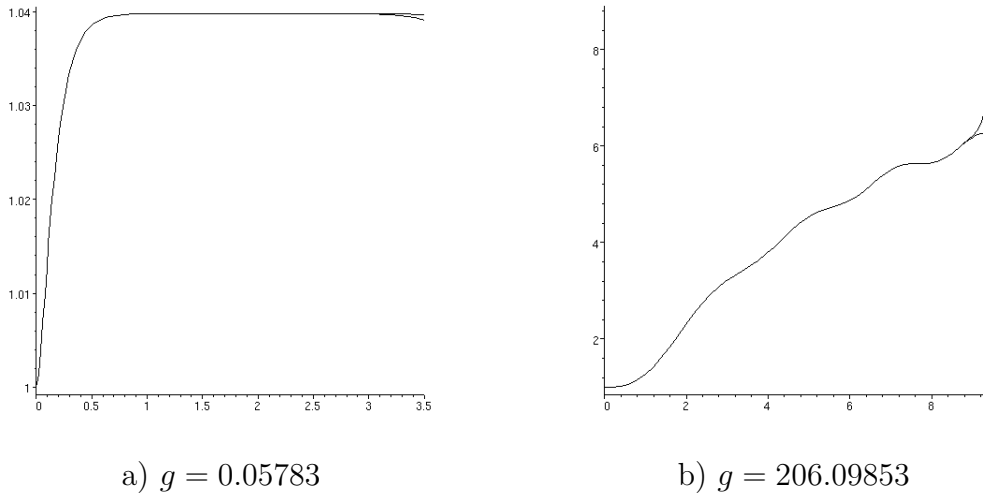


Figure 2. Plot of $L_{30}(\lambda)$ and $L_{29}(\lambda)$ with $\alpha = \alpha_M$

efficient method in which the singularity contribution is absent. We will therefore be able to calculate the infinite coupling limit. This is something that cannot be done via resummation of the Bender Wu expansion.

3. Semi Classical Expansion

In this section we resum a semi classical expansion in \hbar for the a_n coefficients in W . We write $\Psi = e^{W/\hbar}$ and consider the modified differential equation

$$-\hbar^2 \frac{d^2 \Psi}{dx^2} + (b_0 + b_1 x^2 + b_2 x^4) \Psi = 0. \quad (10)$$

The original problem (1) in which $\hbar = m = 1$ is then recovered via a rescaling $x \rightarrow cx$ provided

$$E = -b_0 \frac{c^2}{\hbar^2}, \quad 1 = b_1 \frac{c^4}{\hbar^2}, \quad g = b_2 \frac{c^6}{\hbar^2}. \quad (11)$$

We substitute Ψ into the \hbar dependent differential equation to generate relations between the a_n . The equivalent expressions to (7) are

$$b_0 = 2a_1 \hbar, \quad b_1 = 4a_1^2 + 12a_2 \hbar, \quad b_2 = 16a_1 a_2 + 30a_3 \hbar \quad (12)$$

and the new version of (8) is

$$2\hbar(n+1)(2n+1)a_{n+1} + \sum_{m=1}^n 4m(n-m+1)a_m a_{n-m+1} = 0. \quad (13)$$

The advantage of performing this rescaling is that we now have some freedom to choose a_1 and a_2 . We will restrict the choice however by requiring $\hbar \geq 0$ with both c and \hbar real. This will allow us to choose a_1 and a_2 up to a sign. We will choose $a_1 = -1/2$ and $a_2 = -1/8$. We showed that this was the appropriate sign choice in [1] to ensure that

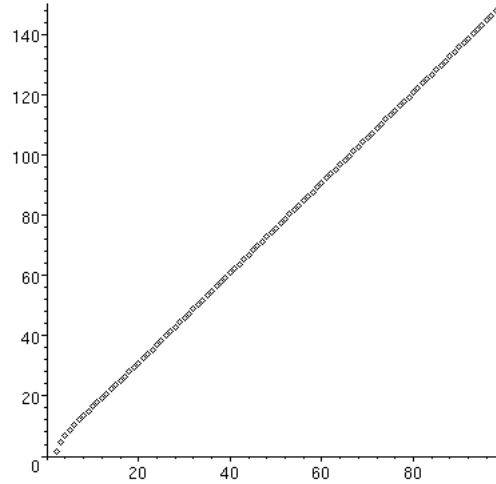


Figure 3. Ratio of coefficients of \hbar^n in b_2

the boundary condition (2) is satisfied. With these choices we can reduce (11) and (12) to

$$E = \frac{1}{\sqrt{1 - \frac{3}{2}\hbar}}, \quad g = \hbar b_2 E^3. \quad (14)$$

We now assume an expansion $a_n = \sum_{m=0}^{\infty} a_{n,m} \hbar^m$ for each $n \geq 3$. This is substituted into (13) and coefficients of \hbar^m compared for each n . We first compare coefficients of \hbar^0 to get the $a_{n,0}$ then the coefficients of \hbar^1 give the $a_{n,1}$ etc. At each stage previous results are substituted into the new equation. By continuing this process sufficiently many times we can find each a_n to any order required. A simple program can therefore be created to calculate b_2 (by using the \hbar expansion of a_3) as an expansion in \hbar . The first few orders are

$$b_2 = 1 + \frac{5}{8}\hbar - \frac{35}{32}\hbar^2 + \frac{2555}{512}\hbar^3 - \frac{69545}{2048}\hbar^4 + \frac{4849705}{16384}\hbar^5 - \frac{202337485}{65536}\hbar^6 + \dots \quad (15)$$

The expansion of b_2 in \hbar is an alternating sign series so we plot the ratio of successive coefficients of \hbar^n in b_2 in such a way that we are dividing by the preceding term and removing the minus sign. We illustrate this in figure 3 for the first 100 coefficients and note the approximate linear behaviour for large orders. This suggests the asymptotic behaviour of the coefficients in b_2 have the form $(-1)^{n+1} k_1^n \Gamma(n + k_2)$ where k_1 and k_2 are real constants. Such asymptotic expansions have a zero radius of convergence as demonstrated via the alternating sign series test.

We shall therefore resum (15) for a particular $s_0 \equiv 1/\hbar$ from which E and g can be calculated. The c_n in $L_N(\lambda)$ now correspond to the coefficients of \hbar^n in the b_2 expansion. We note that $\hbar = 0$ corresponds to $g = 0$ and $E = 1$ whilst $\hbar \rightarrow 2/3$ corresponds to $g \rightarrow \infty$. We actually find that $\hbar \in [0, 2/3)$ corresponds to $g \in [0, \infty)$ which can be confirmed by the results of [1]. We therefore calculate some couplings and energy eigenvalues within this range. The results are given in figure 4 again compared

\hbar	α_M	λ_M	\mathbf{b}_2	\mathbf{g}_{est}	\mathbf{g}_{best}	Err ($10^{-4}\%$)
0.05	1.5190	3.5078	1.0289799	0.0578315	0.0578320	8.85
0.10	2.2473	8.4878	1.0546589	0.1345810	0.1345815	3.68
0.15	2.5696	11.0496	1.0780575	0.2370176	0.2370183	2.69
0.20	2.7754	12.7628	1.0997450	0.3755562	0.3755570	2.20
0.25	2.8514	13.2331	1.1200769	0.5667191	0.5667201	1.83
0.30	2.8555	13.0189	1.1392958	0.8379415	0.8379430	1.71
0.35	2.8557	12.8266	1.1575774	1.2375925	1.2375945	1.66
0.40	2.8557	12.6736	1.1750540	1.8579236	1.8579267	1.65
0.45	2.8557	12.5499	1.1918288	2.8946853	2.8946902	1.70
0.50	2.8557	12.4457	1.2079838	4.8319353	4.8319442	1.83
0.55	2.8557	12.3584	1.2235859	9.1926365	9.1926555	2.07
0.60	2.8557	12.2820	1.2386905	23.5024991	23.5025564	2.44
0.65	2.8557	12.2158	1.2533439	206.0979166	206.0985278	2.97

Figure 4. Results of resummation in the semi classical expansion

to results, g_{best} (accurate to the stated number of significant figures) generated from [1]. The energy eigenvalues produced are exact however it is the coupling that we are trying to approximate via the resummation process. We note that errors in the coupling are in the order of $10^{-4}\%$. Most importantly however the error remains within this order of magnitude for the full spectrum of \hbar in contrast to resummation in the coupling. We can attribute this success to the fact that $\hbar \in [0, 2/3)$ as opposed to $g \in [0, \infty)$ and the resummation process being most effective for small \hbar or g . Also we encountered difficulties in resumming the coupling expansion for large g due to the singularity at the origin in the s plane. This problem has been removed in the semi classical expansion.

For higher \hbar we expect the error to be greater since the contribution from singularities increases. It is interesting to note however that whilst this is true for the larger values of \hbar , the highest error is when $\hbar = 0.05$. We attribute this to an insufficiently large value of P . We plot $L_{30}(\lambda)$ and $L_{29}(\lambda)$ in figure 5a with $P = 50$ and note the decaying behaviour of the curves. With $P = 100$ say we recover the expected behaviour of a flattening curve followed by the divergence of the two curves. One curve increases whilst one decreases from the point of divergence as illustrated in figure 5b. This is because the expansion of $(s - s_0^{1/\alpha})^{-1}$ in powers of $s_0^{1/\alpha}/s$ is only valid for large s . Whilst this is a valid assumption given the contour of integration, the series does require more terms to achieve a suitable level of approximation when s_0 becomes larger or equivalently \hbar becomes smaller. The error as a result of truncation in this expansion is systematic hence the decaying nature of the curve for larger values of λ . This effect becomes more pronounced for larger α . It is possible that α becomes sufficiently large to cause this decaying behaviour before singularity contributions becomes significant. However in this case the curve will still fail the monotonic condition. We resultingly

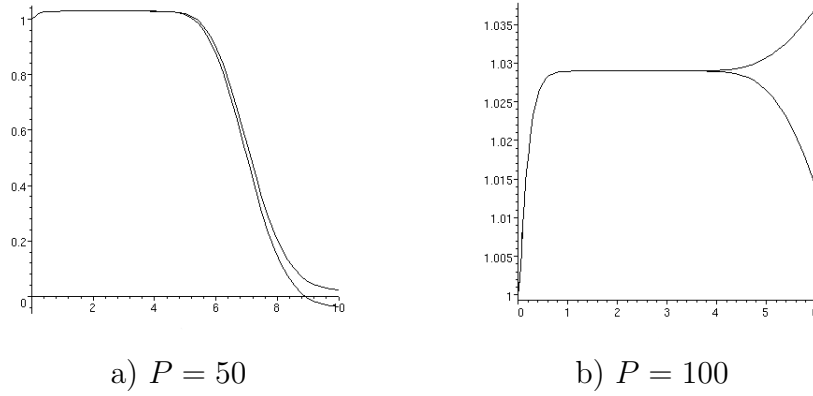


Figure 5. Plot of $L_{30}(\lambda)$ and $L_{29}(\lambda)$ with $\hbar = 0.05$

take both a smaller α and a smaller λ and therefore get greater singularity contributions than if we had taken a larger P . Despite the improvement expected with larger P we are still able to extract good approximations with $P = 50$.

The case $\hbar \rightarrow 2/3$ is particularly interesting because this corresponds to the infinite coupling limit. With $E_\infty = (3/b_2(2/3)/2)^{1/3}$ this limit corresponds to $E \rightarrow E_\infty g^{1/3}$. Using our resummation method we find $E_\infty = 1.0603632150$ compared to the value $E_\infty = 1.06036209$ which is exact to the stated number of significant figures. That is an error of approximately $1.06 \times 10^{-4}\%$. Parisi [19] was also able to calculate this limit as $E_\infty = 1.06038$.

The method outlined so far for the ground state can be generalised to find the energy and wavefunctions of the excited states. We write the q th excited state $\Psi = P_q \Psi_0$ with energy $E = E_q + E_0$. Now consider

$$- \hbar^2 \frac{d^2 \Psi}{dx^2} + (b_0 + b_3 + b_1 x^2 + b_2 x^4) \Psi = 0 \quad (16)$$

which using (10) reduces to

$$- \hbar^2 \frac{d^2 P_q}{dx^2} - 2W' \hbar \frac{dP_q}{dx} + b_3 P_q = 0. \quad (17)$$

We scale $x \rightarrow cx$ to recover the AHO oscillator (1) provided that in addition to (14) we also have

$$E_q = - \frac{b_3 c^2}{\hbar^2} = - \frac{b_3}{\hbar} E_0 = - \frac{b_3}{\hbar \sqrt{1 - \frac{3}{2}\hbar}}. \quad (18)$$

We now need to find b_3 and U_q using (17) which is easily done using a similar approach to that described for the ground state. That is expand

$$U = \sum_{n=0}^{\infty} \sum_{m=0}^{\infty} c_{n,m} \hbar^m x^n, \quad (19)$$

$$b_3 = \sum_{m=0}^{\infty} b_{3,m} \hbar^m, \quad (20)$$

and substitute into (17). By comparing coefficients of \hbar^k and x^n we get

$$\begin{aligned}
& - \sum_{i=0}^k b_{3,i} c_{n,k-i} + (n+2)(n+1)c_{n+2,k-2} \\
& + 4 \sum_{m=1}^{(n+1)/2} \sum_{i=0}^{k-1} m(n+2-2m)a_{m,i}c_{n+2-2m,k-i-1} = 0
\end{aligned} \tag{21}$$

for $k > 1$. The $k = 0$ case reveals $b_{3,0} = 0$ or $c_{0,n} = 0$ for all n . Clearly the former is required. The $k = 1$ case is given by

$$- b_{3,1}c_{n,0} + 4\hbar \sum_{m=1}^{(n+1)/2} m(n+2-2m)a_{m,0}c_{n+2-2m,0} = 0. \tag{22}$$

We consider this equation for each n starting with $n = 0$ and find at each stage that $c_{n,0} = 0$ until we reach a point where

$$b_{3,1} = 4na_{1,0} = -2n. \tag{23}$$

Clearly $b_{3,1} = 0$ is required for the ground state, $q = 0$. Note also that a Taylor expansion of (18) would reveal $b_{3,1} = E_{q,0}$. This corresponds to the q th harmonic oscillator with energy eigenvalues $E = 2q + 1$ or $E_{q,0} = 2q$. So we have $c_{n,0} = 0$ for $n < q$ and $b_{3,1} = 2q$.

We can fix one of the x^n coefficients in U_q by a choice of normalisation and therefore set $c_{q,0} = 1$ with the remaining $c_{q,n} = 0$. Now consider the $k = 2$ case for each n then $k = 3$ etc. We see that at each stage (21) can be solved for $c_{n,k-1}$ provided $n \neq q$ or if $n = q$ we get $b_{3,k}$.

By solving a series of linear equations we have managed to determine b_3 and U_q and hence found the excited wavefunctions and energies up to any order required. We can then apply our resummation method to evaluate the series expansion.

One advantage of this method is that we can calculate the energy eigenvalues for an infinite coupling. We have already seen that this is given when $\hbar = 2/3$. By using (18) and (14) we can write

$$E_q = -\frac{b_3}{\hbar} \left(\frac{g}{\hbar b_2} \right)^{\frac{1}{3}}. \tag{24}$$

So in the infinite coupling limit, $\hbar \rightarrow 2/3$ we have $E_q = E_{q,\infty}g^{1/3}$ where

$$E_{q,\infty} = -\frac{3}{2}b_3(2/3)E_{0,\infty}. \tag{25}$$

Applying our resummation method we can calculate b_3 and hence $E_{q,\infty}$. A table listing the first ten b_3 is given in figure (6).

4. Tuning the Boundary Condition

In this section we use our resummation technique to try and explain why the method for generating energy eigenvalues in [1] is so efficient. In this approach we examine the large x behaviour of $W = \sum_{n=1}^{\infty} a_n x^n$ by applying the resummation technique already

\mathbf{q}	$\alpha_{\mathbf{M}}$	$\lambda_{\mathbf{M}}$	\mathbf{b}_3^{est}	\mathbf{b}_3^{best}	Error (%)
1	3.3554	17.9902	-1.722251	-1.722249	0.0001
2	3.2057	15.4576	-4.020691	-4.020850	0.0040
3	3.1254	13.8688	-6.654020	-6.654572	0.0083
4	3.0734	12.7075	-9.555955	-9.557404	0.0152
5	3.0341	11.7759	-12.681877	-12.686239	0.0344
6	3.0046	11.0209	-16.000874	-16.012209	0.0708
7	2.9831	10.4064	-19.489826	-19.514237	0.1251
8	2.9675	9.8993	-23.130233	-23.176133	0.1980
9	2.9560	9.4721	-26.906049	-26.984993	0.2926
10	2.9473	9.1068	-30.803510	-30.930247	0.4098

Figure 6. Infinite coupling values of b_3

outlined. The differential equation implies large x asymptotic behaviour of the form $W \sim \pm\sqrt{g}x^3/3$ and (2) then requires us to take the solutions that have a negative sign. We again employ Cauchy's theorem defining

$$T(\lambda) = \frac{1}{2\pi i} \frac{1}{\lambda^3} \int_C ds \frac{e^{\lambda s}}{s} W(s). \quad (26)$$

so that when the boundary condition is satisfied we have $\lim_{\lambda \rightarrow \infty} T(\lambda) = -\sqrt{g}/18$ provided W has no singularities in the right half $s \equiv 1/x$ plane.

In the case of the quartic anharmonic oscillator, W exhibits analytic behaviour in the whole complex s plane however with higher order polynomial potentials this is not the case. A prescription in which we take $W(s) \rightarrow W(s^\alpha)$ and $1/\lambda^3 \rightarrow 1/\lambda^{3\alpha}$ in (26) was introduced. By reducing $\alpha < 1$ singularities are rotated into the half plane $\Re(s) < 0$ in which case they become exponentially suppressed. Since we will restrict ourselves to the quartic oscillator in this paper we shall take $\alpha = 1$.

A rescaling $x \rightarrow cx$ ($c \in \mathbb{R}$) in the differential equation allows us to fix the ratio $k \equiv a_1/a_2 = \pm 4$. We make a choice for a_2 and sign of k then solve the remaining a_n in terms of a_3 via the recurrence relation (8). We vary a_3 until we observe the correct boundary condition in $T(\lambda)$. As with the previous direct resummation methods we use a truncated expansion of W to approximate $T(\lambda)$ with $T_N(\lambda)$.

When $T_N(\lambda)$ is plotted for a_3 too small to satisfy the boundary condition, we find a rapidly decreasing curve. If a_3 is too large then we find a rapidly increasing curve. We are therefore able to tune a_3 by adjusting upper and lower bounds to find an interval within which a_3 lies. We start with a modest value of N and tune a_3 until $T_N(\lambda)$ produces a curve flattening for the larger values of λ . The range of λ considered should be chosen to ensure T_N is a good approximation to T . That is up to a value of λ at which T_N and T_{N-1} appreciably diverge. To further increase the level of accuracy we need to consider whether the curve is rapidly increasing or decreasing for larger values of λ . We therefore need to increase N . So N effectively determines the level of accuracy.

With the sign choice of k and value of a_2 , a_3 is determined up to an arbitrary level of accuracy. The physical parameters are then found via

$$E = \frac{-2ka_2}{(16ka_2^2 + 30a_3)^{\frac{1}{3}}} g^{\frac{1}{3}} \quad (27)$$

$$\rho = \frac{4k^2a_2^2 + 12a_2}{(16ka_2^2 + 30a_3)^{\frac{2}{3}}} g^{\frac{2}{3}}. \quad (28)$$

The procedure can be generalised to find the excited energy eigenvalues. As with the semi classical expansion we write the q th excited state $\Psi_q = P_q\Psi_0$ and energy $E = E_0 + E_q$. Then P_q is expanded in powers of x , $P_q = \sum_{n=0}^{\infty} c_n x^n$. The even powered coefficients are set to zero for q odd and the odd powered coefficients to zero for q even. Again we used a scaling of the differential equation $x \rightarrow cx$ and substitute in Ψ_q . We compare coefficients of x^n to get a recurrence relation for the c_n . This also determines E_q in terms of the c_n . We set the first non zero coefficient in the expansion (c_0 or c_1) to unity and use the recurrence relation to solve the c_n in terms of c_2 or c_3 . We now define U via

$$U(\lambda) = \frac{1}{2\pi i} \int_C ds \frac{e^{\lambda s}}{s} P_q(s^\alpha) \quad (29)$$

and use the truncated expansion for P_q to approximate $U(\lambda)$ with $U_N(\lambda)$.

We vary either c_2 or c_3 as before and again observe the rapidly increasing or decreasing behaviour for solutions which do not correspond to eigenstates. For example in the odd case we vary $\tau = -c_3$. There will be multiple values of τ which correspond to different levels of excitation. We label these τ_n such that $\tau_{n+1} > \tau_n$. With $\tau < \tau_1$, $U(\lambda)$ corresponds to a rapidly increasing curve and with $\tau_1 < \tau < \tau_2$ we get a rapidly decreasing curve. With $\tau_2 < \tau < \tau_3$ $U(\lambda)$ switches back to a rapidly increasing curve. This switch between rapidly increasing and rapidly decreasing occurs whenever we increase τ past one of the τ_n . The level of truncation determines the level of accuracy as before.

Although the ground state was analytic in the whole complex s plane for the quartic oscillator we found that the excited states were not. Therefore when we tune the curve, we get oscillations instead of a flattening behaviour. We could in principal use our technique of decreasing $\alpha < 1$ to move the poles into the left half plane where they are suppressed by the exponential factor. This reproduces the flattening behaviour of the $T_N(\lambda)$ curve. We find however that it suffices to tune for the oscillations.

One of the advantages of this approach compared to direct resummation of a perturbative expansion in \hbar or g is that we are able to produce solutions in which $\rho < 0$. These solutions are dominated by instanton effects which are non perturbative in both \hbar and g . Also this process allows us to determine an energy eigenvalue to an arbitrary level of accuracy. It is the switch between the rapidly increasing or decreasing behaviour of T_N or U_N that makes this method work so well. In [1] we postulated a reason for this and in this section we use our resummation techniques to further investigate this behaviour.

4.1. The Ground State - Zeros, Poles and Cuts

If we solve the differential equation (1) for its large positive x behaviour without the boundary condition (2) we find two asymptotic solutions, $W = \pm\sqrt{g}x^3/3$. The general large x solution to (1) is therefore of the form

$$\Psi_l = \exp\left(-\frac{\sqrt{g}}{3}x^3\right) + A \exp\left(\frac{\sqrt{g}}{3}x^3\right). \quad (30)$$

The boundary condition (2) however requires us to take $A = 0$. Ψ_l in general has zeros at specific points in the complex x plane depending on A . The only exception to this is when $A = 0$ at which point we only asymptotically approach zero as $x \rightarrow \infty$. For $A < 0$ these zeros lie along the real axis whereas for $A > 0$ they lie off the real axis, somewhere in the complex x plane. There will also be contours in the complex x plane along which Ψ_l is purely real and negative. The zeros and negative regions in Ψ_l will be manifested as cuts and poles in $\log \Psi_l$.

It is clear that any pole or cut in the right half complex x plane would result in an exponentially increasing or decreasing $L_N(\lambda)$. Oscillations will occur due to a pole lying off the real axis however we took modest N to ensure we only see the beginning of the oscillation and hence the appearance of a rapidly increasing or decreasing curve. We hypothesised in [1] that this is what is being observed in $L_N(\lambda)$. In this section we present numerical evidence to support this. We are essentially tuning the solution until $A = 0$. For $A \neq 0$ the resummation is conveniently spoilt in such a way that we are able to refine the solution. In this section we will employ Cauchy's theorem to determine the location of zeros in the solutions to the differential equation as constructed in the previous section. We will then be able to observe the dependence of these zeros on a_3 . Whilst we have so far only presented an argument based on the large x behaviour of Ψ we will find that the location of zeros in Ψ_l do indeed correspond approximately to the location of zeros in the full solution.

We note that since the coefficients a_n in W (and a Taylor expanded W_l) are all real, any cut or pole in the upper half s plane should necessarily be mirrored in the lower s plane. Let us momentarily assume that in the right half s plane $W(s)$ only contains poles located at s_p and s_p^* . We then construct

$$\begin{aligned} S(\lambda) &= \frac{1}{2\pi i} \int_C ds \frac{e^{\lambda(s-s_0)}}{s-s_0} W(s) \\ &\sim W(s_0) + c \cos(\lambda s_p^{\Im} + \nu) e^{\lambda(s_p^{\Re} - s_0)} \end{aligned} \quad (31)$$

where c, ν are real numbers and s_p is split into real and imaginary parts, $s_p^{\Re} + i s_p^{\Im}$. If we had included a cut contribution instead of a pole then we would expect contributions from the whole cut with each portion of the cut weighted by the exponential factor. In Ψ_l the zero lies on the right end of a region of negativity corresponding to a potential cut in W_l and therefore is the dominant singularity contribution in our contour integral if $W = W_l$. So whilst $W(s)$ does not necessarily have just one pole in the positive right quadrant we will model the cuts by a pole representing a weighted average. Since the

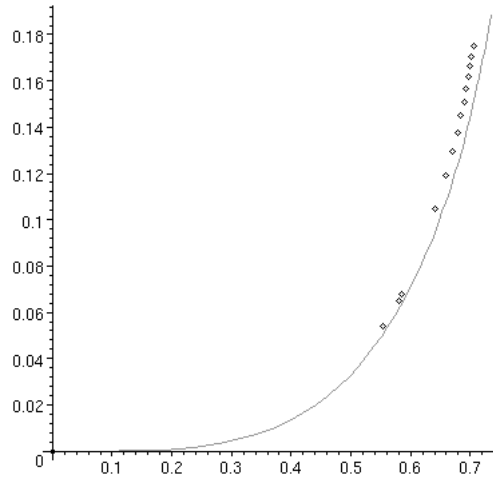


Figure 7. Location of zeros

zero is the dominant contributor we will find that $S(\lambda)$ at least in the case of W_l allows us to reasonably approximate the location of our zero. We will apply this model to our original Ψ and predict zeros close to the zeros of Ψ_l . As usual we use the truncated expansion of W to approximate $S(\lambda)$ by $S_N(\lambda)$.

With the above construction we are in a position to numerically determine the location of the conjugate poles. Initially we will assume that $s_p^{\Im} \neq 0$ and plot $S_N(\lambda)$ for a given s_0 . We expect to see oscillations in the curve either growing ($s_p^{\Re} > s_0$), decaying ($s_p^{\Re} < s_0$) or fixed in amplitude. We tune s_0 until we achieve the latter at which point we have $s_p^{\Re} = s_0$. With this s_0 we can determine the frequency of the oscillations in $S_N(\lambda)$, this gives us s_p^{\Im} .

If we do not observe the oscillatory behaviour in $S_N(\lambda)$ even with N, P sufficiently large then it may be that $s_p^{\Im} = 0$. If this is the case then we use $S_N(\lambda)$ to approximate $W(s_0)$ for $s_0 > s_p$. As s_0 becomes closer to s_p however the effect of our pole becomes more significant since the exponential dampening factor becomes reduced. We must therefore take larger λ which in return requires larger N . Alternatively we can try increasing $\alpha > 1$. This causes the final term in S_N to be reduced in comparison to the penultimate term due to the Γ function. This again allows a larger λ and hence greater exponential dampening. Ultimately though we are unable to extract $W(s_0)$ from $S_N(\lambda)$ for $s_0 \leq s_p$ and indeed the process becomes more difficult as s_0 approaches s_p . We can however determine s_p by approximating Ψ to a linear behaviour in this region. We justify this by solving the differential equation in a region where W' and W'' are more dominant than any potential term. Numerically this linear behaviour appears to work well at least within the region that we were realistically able to plot.

For a_3 too small we find that the zeros lie along the real s axis with zeros approaching $s = 0$ (i.e. $x = \infty$) and indeed attaining this value as a_3 becomes appropriate for the correct boundary condition to be satisfied. For a_3 too large we find that the location

of zeros lie off the real axis and into the complex plane. They appear to lie on some contour which approaches $s = 0$ as a_3 approaches its correct value. We plot the location of some of these complex zeros of Ψ in figure 7§. We have restricted this plot to one quadrant only however the plot would necessarily be mirrored into all four quadrants. The solid line represents the location of zeros of Ψ_l as constructed at the beginning of this section.

We note that the two sets of zeros are not in exact agreement although there does appear to be a correlation. We attribute the differences largely due to Ψ_l being a small s approximation and we therefore expect the approximation to improve as $|s| \rightarrow 0$ which appears to be happening in the plot. Unfortunately it becomes increasingly difficult to numerically calculate zeros of Ψ as we get closer to the origin since the period of oscillation becomes very large. In order to measure this period we need to be able to plot at least the first few oscillations. This requires an increasingly large λ which in turn increasingly requires a large number of terms.

We also question how accurately our numerical technique can accurately determine the location of zeros. As an example we calculate analytically the location of the zeros in $\Psi = \exp(x^3) + \exp(-x^3)$. Applying the resummation process to $\log(\Psi_t)$ expanded in positive powers of x we are able to numerically calculate the location of the zero. We find analytically that a zero exists at $0.745 + 0.43i$ whereas numerically we find it exists at $0.738 + 0.429i$. Given the scale of the plot this error is relatively insignificant.

4.2. Excited States - Large x behaviour

We substitute $\Psi_q = P_q \Psi_0$ into the differential equation (1) to produce a new differential equation satisfied by P_q ,

$$\frac{d^2 P}{dx^2} + 2 \frac{dW}{dx} \frac{dP_q}{dx} + E_q P_q = 0. \quad (32)$$

Taking $W \sim -\sqrt{g}x^3/3$, this differential equation exhibits two types of large x asymptotic solution

$$P \sim \exp\left(-\frac{E_q}{2\sqrt{g}x}\right) \quad \text{or} \quad P \sim \exp\left(\frac{2\sqrt{g}x^3}{3}\right). \quad (33)$$

We necessarily choose the first of these to ensure the boundary condition (2) is satisfied. When the boundary condition is satisfied $U_N(\lambda)$ produces a flat curve (having adjusted α appropriately) which would be expected if we have correctly chosen the large asymptotic behaviour. If the second type of asymptotic behaviour is chosen then we would expect to observe a correction to $T_N(\lambda)$ due to a singularity at $s = 0$. We hypothesised in [1] that when c_2 or c_3 does not correspond to an energy eigenstate then we are observing the second type of asymptotic large x behaviour.

Using the resummation technique already outlined, the prefactors corresponding to different levels of excitation may be plotted. The prefactors corresponding to the 1st,

§ We have actually scaled the complex plane so that $s^3 \rightarrow \sqrt{16a_1a_2 + 30a_3s^3}/3$ for simplicity of calculation in figure 7

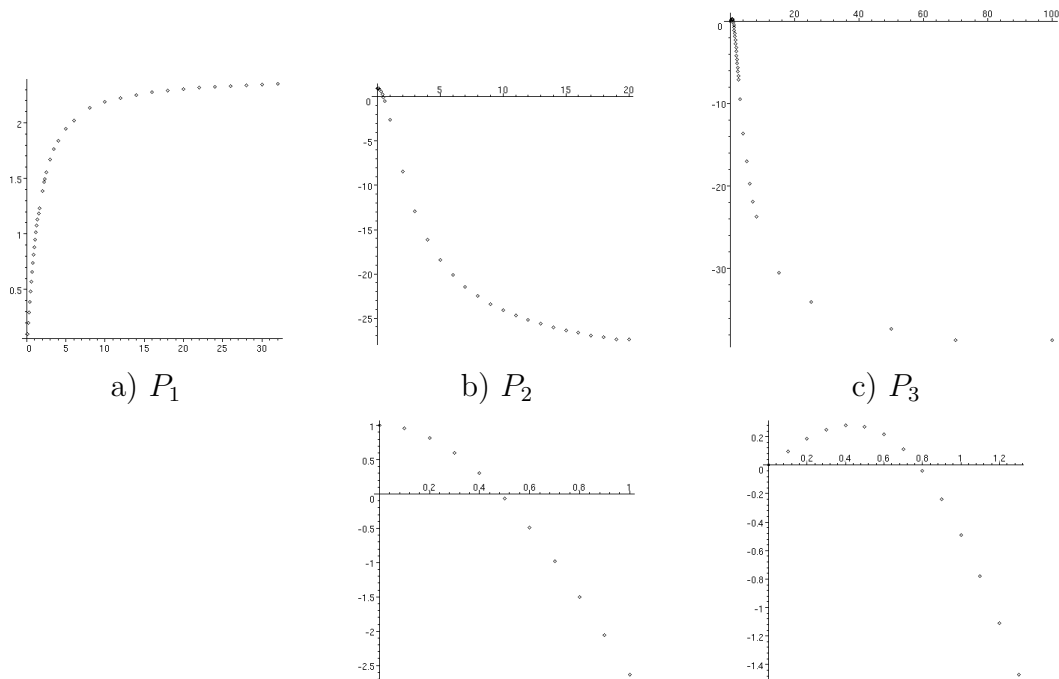


Figure 8. Prefactors corresponding to the first three excitations

2nd and 3rd excited states are shown in figure 8 both on a large and small x scale. Since these functions are either odd or even we restrict the domain to $x \geq 0$. As would be expected the prefactor corresponding to the first excited state has one zero located at the origin. The 2nd excited state has two zeros and the 3rd excited state has 3 zeros when considered along the whole of the real axis. The tuning procedure did not provide a method for determining which level of excitation we have, just that we had determined an energy eigenstate. Using our resummation method to plot the prefactor we are able to confirm which energy eigenstate has been found by counting the number of nodes. The technique in section 3 provides an alternative method. We could use resummation in a \hbar expansion to approximate c_2 or c_3 and then use the tuning method to determine the value more accurately.

We note that for large x these prefactors asymptotically approach some constant value as predicted. For example the prefactor corresponding to some energies either side of the first excited state energy level are shown in figure 9. For $\tau_1 < \tau < \tau_2$ we see that P quickly becomes very large. This is similarly true for $\tau < \tau_1$ however this time P becomes large in the negative direction. This appears not to be the result of a pole or cut otherwise for large x the resummation technique would exhibit singularity contributions. Instead we find the prefactor is simply resumming to large values and these values are increasing in size rapidly. We test the hypothesis that we are observing prefactors with large x behaviour determined by the second type of asymptotic behaviour in (33) by

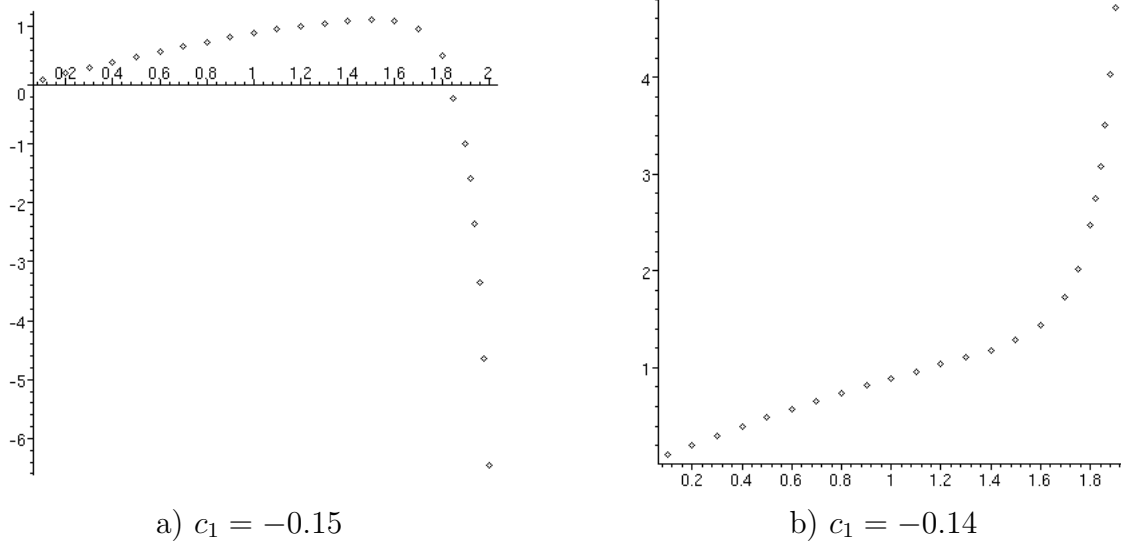


Figure 9. P for values of c_1 either side of $e_1 = -0.1458432840772$

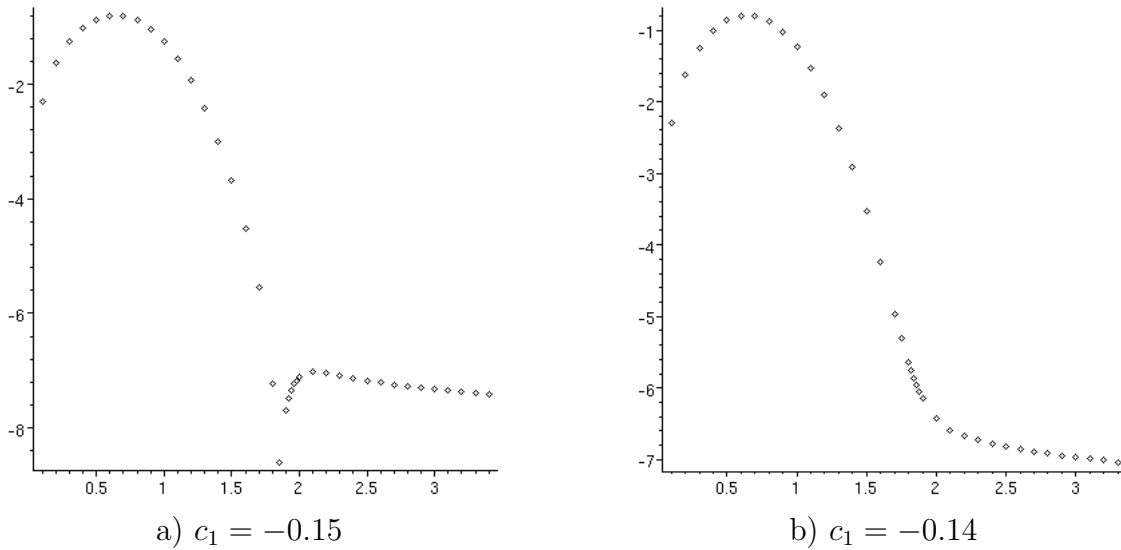


Figure 10. Q for values of c_1 either side of $\tau_1 \approx -0.1458432840772$

plotting

$$Q \equiv \log |P| - \frac{2}{3}\sqrt{g}x^3. \tag{34}$$

If the hypothesis is correct then we expect Q to approach a constant for large x . We plot these graphs for those same values of c_1 as before and display them in figure 10. As predicted these plots do flatten out for large x at least on the scale of $\exp(x^3)$. This numerically supports our hypothesis.

5. A Shifted Expansion

Let us momentarily remove α from $L(\lambda)$ by setting $\alpha = 1$. We were unable to directly evaluate $L(\lambda)$ even having replaced $f(s)$ with the truncated asymptotic expansion. This was due to the $s - s_0$ denominator in the integrand which we expanded to give a sum of integrals of the form

$$\int_C ds \frac{e^{\lambda s}}{s^n} = \frac{\lambda^n}{\Gamma(n)} \quad (35)$$

which are more easily evaluated. Unfortunately the expansion of this denominator required summing over two variables in $L_N(\lambda)$. We truncated the expansion of the $(s - s_0)^{-1}$ term to a relatively high order to avoid complications arising from a truncated form of this expansion. This effectively meant we had to compute a series involving a sum of NP terms. With our chosen N and P this amounted to 1500 terms.

Instead we shall briefly investigate the possibility of shifting $s \rightarrow s + s_0$ in $L(\lambda)$ and then using the truncated expansion of $f(s)$ to approximate $L(\lambda)$. That is we write

$$f(s + s_0) = \sum_{n=0}^{\infty} \frac{c_n}{(s + s_0)^n} = \sum_{n=0}^{\infty} \frac{\tilde{c}_n}{s^n} \quad (36)$$

by expanding the $(s + s_0)^{-n}$ terms in powers of s_0/s . Our new coefficients \tilde{c}_n would then be dependent on s_0 so a separate expansion would be required for each s_0 we try to evaluate.

We then truncate the new expansion and substitute into $L(\lambda)$. Having done this we reinsert the parameter α with the substitution $s \rightarrow s^\alpha$.

$$L_N(\lambda) = \sum_{n=0}^N \tilde{c}_n \frac{\lambda^{\alpha n}}{\Gamma(\alpha n)}. \quad (37)$$

The advantage of this type of expansion is that we no longer need to worry about a double summation truncated to order N and P . This reduces the computational time to evaluate the series but also prevents the problems encountered in 3 as a result of truncation in P .

We should note however that the α parameter in the original L_N (5) is different to the α in (37). In the original formulation α caused singularities to be rotated about the origin. This is still the case in the new formulation however we now have a different origin since s has been shifted. It will depend on the location of singularities as to which method will allow a larger α and therefore better dampening of pole contributions.

We complete our resummation process using the shifted \hbar expansion and present the results in figure 11. We note that the errors are considerably larger than in the previous method. So whilst this method does have some advantages it is clearly less efficient for the semi classical expansion. We attribute this to the different geometry involved when rotating poles by varying α . It is clear that in the shifted method we have smaller values of α_M and therefore λ_M which results in less dampening of any pole contributions. Although this method is inferior for the expansion of b_2 we should

\hbar	α_M	λ_M	\mathbf{b}_2	\mathbf{g}_{est}	\mathbf{g}_{exact}	Err (%)
0.05	1.0000	0.5166	1.0289943	0.0578329	0.0578320	0.002
0.10	1.0040	0.5631	1.0545995	0.1345734	0.1345815	0.006
0.15	1.0627	0.7669	1.0791362	0.2372547	0.2370183	0.100
0.20	1.0971	0.9049	1.1021792	0.3763874	0.3755570	0.221
0.25	1.1303	1.0487	1.1244110	0.5689119	0.5667201	0.387
0.30	1.1569	1.1569	1.1457268	0.8426714	0.8379430	0.564
0.35	1.1832	1.3033	1.1665395	1.2471800	1.2375945	0.775
0.40	1.2060	1.4223	1.1866922	1.8763800	1.8579267	0.993
0.45	1.2264	1.5340	1.2062905	2.9298231	2.8946902	1.214
0.50	1.2435	1.6317	1.2252384	4.9010160	4.8319442	1.429
0.55	1.2625	1.7442	1.2441147	9.3469363	9.1926555	1.678
0.60	1.2777	1.8371	1.2622842	23.9503681	23.5025564	1.905
0.65	1.2941	1.9401	1.2803813	210.5377762	206.0985278	2.154

Figure 11. Results of resummation in the shifted semi classical expansion

note that depending on the location of singularities it may prove to be better in other expansions and therefore should not be ignored.

We could question however whether it is fair to compare this method with $N = 30$ to the previous method which effectively had $NP = 1500$ terms. In the shifted example we could afford to take more terms given the reduced computational power required to perform the resummation. We note however that in some perturbative expansions calculating an expansion to higher orders can often be the limiting factor.

6. Error Estimates

There are two main sources of error in our prescription for evaluating $f(s_0)$. The first is due to $L_N(\lambda)$ only being an approximation to $L(\lambda)$. We require $L_N(\lambda)$ to differ from $L_{N-1}(\lambda)$ by no more than say σ percent. Therefore we can think of σ as being an error. Smaller σ requires evaluating $L(\lambda)$ for a smaller λ which has the unwanted side effect of reducing the exponential dampending of any singularities of $f(s)$ in the left half plane. This is the second source of error. We shall outline a method for estimating the error in $L(\lambda)$ as a result of singularity contributions.

Consider a pole of $f(s)$ located at s_p . We will only be working with asymptotic expansions for which all coefficients, a_n are real. This implies that for a pole to exist at s_p we must necessarily have a pole at the conjugate location s_p^* . We shall for now assume that $f(s)$ has just one pair of poles in the left half s plane but is analytic on the remainder of the complex plane. The pair of conjugate poles gives a contribution to (4) of the form

$$c \cos(\lambda y_p + \nu) e^{\lambda(x_p - s_0^{1/\alpha})} \quad (38)$$

where $s_p^{1/\alpha}$ is split into real and imaginary parts $s_p^{1/\alpha} = x_p + iy_p$ and c, ν are real numbers. In the large λ limit this contribution approaches zero provided α is not taken so large as to rotate the poles into the right half plane. For a general α the correction (38) looks like an oscillating curve either growing or decreasing in amplitude. For $x_p > s_0^{1/\alpha}$ the oscillations are growing and for $x_p < s_0^{1/\alpha}$ the oscillations are being damped. We will use this to tune α until the oscillations are fixed in amplitude, say $\alpha = \alpha_T$ at which point $x_p = s_0^{1/\alpha}$. Having determined x_p we determine y_p by calculating the period of oscillations. This is best achieved by considering the λ derivative of $L_N(\lambda)$ and looking for zeros with $\alpha = \alpha_T$. The phase ν and amplitude c are then easily calculated by fixing the location of zeros in the derivative of $L_N(\lambda)$ and also ensuring the correct amplitude of the sinusoidal curve. Now with $\alpha = \alpha_T$ the pole contribution is

$$\frac{e^{\lambda y_p i}}{iy_p} \rho_T + cc = c \cos(\lambda y_p + \nu) \quad (39)$$

where ρ_T is the residue of $f(s^{\alpha_T})$ at s_p^{1/α_T} and cc denotes the complex conjugate. So we have determined ρ_T numerically in terms of the parameters c, y_p and ν .

We want to evaluate $L(\lambda)$ (or $L_N(\lambda)$) when $\alpha = \alpha_M$, the maximal value of α for which the curve is still monotonic. With this value of α the pole contribution is

$$\rho_M \frac{e^{\lambda(s_c - s_0^{1/\alpha_M})}}{s_c - s_0^{1/\alpha_M}} + cc \quad (40)$$

where

$$s_c \equiv \left(s_0^{1/\alpha_T} + iy_p \right)^{\alpha_T/\alpha_M} \quad (41)$$

and ρ_M is the residue of $f(s^{\alpha_M})$ at s_c . We can relate ρ_T and ρ_M via

$$\rho_T = \rho_M \frac{\alpha_M}{\alpha_T} \frac{s_c}{s_p^{1/\alpha_T}} \quad (42)$$

and therefore can calculate the pole contribution from (40). We think of σ as being the error in approximating $L(\lambda)$ with $L_N(\lambda)$ which in this case was chosen to be $\sigma = 10^{-3}\%$ and (40) as being the correction to $L(\lambda)$ as an approximation to $f(s_0)$ as a result of a pole pair contribution.

In general $f(s)$ will not have just one pair of poles but a number of poles and cuts. The contributions from these singularities will be exponentially weighted with singularities lying furthest to the right being most dominant. Due to this exponential weighting a cut contribution will look like a pole dominated by the right most end of the cut. We can therefore apply our procedure assuming the existence of just one pole pair and then interpret the correction (40) as being the dominant or leading order correction. We note however that the right most end of a cut can actually change as it is rotated by increasing α . The left and right ends of a cut may actually switch if α becomes too large. In this case the error estimate may not be the most dominant but will be a more minor correction.

In order to apply our technique we will require sufficient terms to ensure at least two peaks or troughs for $\alpha = \alpha_T$. These must exist within a region where $L_N(\lambda)$ is a

g_{best}	α_T	g_{corr}	Resum Err	Corrected Err	Relative Err
0.057832	1.0000	0.057833	0.00165	0.00002	90
0.134581	1.0040	0.134613	0.00600	0.00023	26
0.237018	1.0627	0.237378	0.09976	0.00152	66
0.375557	1.0971	0.376543	0.22112	0.00263	84
0.566720	1.1303	0.568924	0.38674	0.00389	99
0.837943	1.1569	0.842246	0.56430	0.00514	110
1.237595	1.1832	1.243168	0.77452	0.00450	172
1.857927	1.2060	1.866679	0.99322	0.00471	211
2.894690	1.2264	2.908286	1.21370	0.00470	258
4.831944	1.2435	4.864863	1.42948	0.00681	210
9.192656	1.2625	9.237419	1.67830	0.00487	345
23.502556	1.2777	23.666373	1.90537	0.00697	273
206.098528	1.2941	207.519940	2.15394	0.00690	312

Figure 12. Corrected couplings due to dominant singularity contributions

good approximation to $L(\lambda)$. Clearly $N = 30$ in the Bender Wu expansion is insufficient for large couplings as $L_N(\lambda)$ did not approximate $L(\lambda)$ sufficiently well. We also note that with the semi classical expansion, the errors were of the order $10^{-4}\%$. So in this case the dominant error is provided by σ . In fact the exact values lie between L_{30} and L_{29} in this expansion so σ is actually an error bound. It would however be pointless to calculate the error correction due to singularities without first reducing σ (or N). We will instead apply this technique to the shifted semi classical expansion (section 5). In this technique we found the actual error to be much greater than σ .

We subtract the dominant singularity correction and list the results (g_{corr}) in figure 12. The percentage errors after resummation and percentage errors having subtracted the dominant singularity contribution are listed. The relative error is the ratio of these two errors and indicates that the percentage error has improved by a factor of between 90 and 312. We expect the error as a result of singularities is greater for larger \hbar and this is reflected in these increasing corrections for higher \hbar .

7. Summary

The most impressive application of the modified Borel resummation technique in this paper is not to look for an approximate value of a resummed expansion but instead to use the analytic properties of a function to tune for the correct boundary condition (section 4). This method was first outlined in [1] and in this paper we have given numerical evidence to explain why the technique works. Due to the arbitrary levels of accuracy that may be obtained through this method it is worthy of further study. It has already been applied to anharmonic oscillators with higher order potentials however we believe it may be adaptable to solve other types of problems.

The concept of direct resummation is also important. We have used it to numerically investigate the location of zeros in solutions to the anharmonic differential equation and therefore explain how the tuning technique selects the solution with the correct boundary condition. We found that when the correct boundary condition is not satisfied the logarithm of the wavefunction contains singularities either on the real axis or in the complex plane depending on whether the energy chosen is too large or too small. The existence of these singularities causes an easily observable contribution though the modified Borel resummation procedure in the form of a rapidly increasing or decreasing curve.

In other physical problems we are not always in a position to apply a tuning type method where we look for the correct large x behaviour. We have shown that the modified Borel summation technique can produce reasonably accurate results from perturbative expansions that are ordinarily divergent. This has been shown by considering two different perturbative expansions of the wavefunction. The two expansions have different singularity locations and residues but in both cases these are the half x plane with negative real part. The semi classical expansion in \hbar was particularly useful because it separates the $g^{1/3}$ type behaviour for large g from the expansion we intend to resum. Therefore we get much better results for this part of the spectrum than if we used the Bender Wu coupling expansion.

We have taken the modified Borel technique and improved it by comparing two different methods for approximating the contour integral. Both techniques have their advantages depending on the location of any singularity contributions and how changing the α parameter causes them to move through the complex plane. We have investigated the major sources of error and improved the accuracy of the procedure by subtracting the leading order corrections. Also, in contrast to standard Borel summation we do not require an analytic continuation of the Borel sum since this is encoded in the contour integral.

References

- [1] D. Leonard and P. Mansfield, "Solving the Anharmonic Oscillator: Tuning the Boundary Condition," *J. Phys. A: Math. Theor.* **40** (2007) 10291-10299 [arXiv:quant-ph/0703262].
- [2] P. Mansfield, "The Vacuum functional at large distances," *Phys. Lett. B* **358** (1995) 287 [arXiv:hep-th/9508148].
- [3] P. Mansfield, "Reconstructing the Vacuum Functional of Yang-Mills from its Large Distance Behaviour," *Phys. Lett. B* **365** (1996) 207 [arXiv:hep-th/9510188].
- [4] P. Mansfield, M. Sampaio and J. Pachos, "Short distance properties from large distance behaviour," *Int. J. Mod. Phys. A* **13** (1998) 4101 [arXiv:hep-th/9702072].
- [5] P. Mansfield, "Solving the functional Schroedinger equation: Yang-Mills string tension and surface critical scaling," *JHEP* **0404** (2004) 059 [arXiv:hep-th/0406237].
- [6] H. J. Müller-Kirsten "Introduction to Quantum Mechanics" World Scientific Publishing Co. ISBN 981-256-691-0.
- [7] C. M. Bender and T. T. Wu, "Anharmonic Oscillator," *Phys. Rev.* **184** (1969) 1231.
- [8] B. Simon and A. Dicke, "Coupling Constant Analyticity For The Anharmonic Oscillator," *Annals Phys.* **58** (1970) 76.

- [9] C. M. Bender and T. T. Wu, "Large Order Behaviour Of Perturbation Theory," *Phys. Rev. Lett.* **27** (1971) 461.
- [10] C. M. Bender and T. T. Wu, "Anharmonic Oscillator. 2: A Study Of Perturbation Theory In Large Order," *Phys. Rev. D* **7** (1973) 1620.
- [11] S. Graffi, V. Grecchi and B. Simon, "Borel Summability: Application To The Anharmonic Oscillator," *Phys. Lett. B* **32** (1970) 631.
- [12] J. J. Loeffel, A. Martin, B. Simon and A. S. Wightman, "Pade Approximants And The Anharmonic Oscillator," *Phys. Lett. B* **30** (1969) 656.
- [13] V. Kowalenko and A. A. Rawlinson, "Mellin - Barnes regularization, Borel summation and the Bender asymptotics for the anharmonic oscillator," *J. Phys. A* **31** (1998) L663.
- [14] I. G. Halliday and P. Suranyi, "The Anharmonic Oscillator: A New Approach," *Phys. Rev. D* **21** (1980) 1529.
- [15] R. Balsa, M. Plo, J. G. Esteve and A. F. Pacheco, "Simple Procedure To Compute Accurate Energy Levels Of A Double Well Anharmonic Oscillator," *Phys. Rev. D* **28** (1983) 1945.
- [16] F. M. Fernandez, A. M. Meson and E. A. Castro, "A simple iterative solution of the Schrodinger equation in matrix representation form," *J. Phys. A* **18** (1985) 1389.
- [17] F. Arias de Saavedra and E. Buenda, "Perturbative-variational calculations in two-well anharmonic oscillators," *Phys. Rev. A* **42** (1990) 5073.
- [18] S. Bravo Yuste and A. Martín Sánchez, "Energy levels of the quartic double well using a phase-integral method," *Phys. Rev. A* **48** (1993) 3478.
- [19] G. Parisi, "The Perturbative Expansion And The Infinite Coupling Limit," *Phys. Lett. B* **69** (1977) 329.